Super duplex stainless steels

Article *in* Materials Science and Technology · August 1992

DOI: 10.1179/mst.1992.8.8.685

1 author:

J.-O. Nilsson

50 PUBLICATIONS **1,167** CITATIONS

SEE PROFILE

Overview

Super duplex stainless steels

J.-O. Nilsson

This paper presents an overview of duplex stainless steels (DSS) with particular emphasis on super DSS, i.e. steels containing sufficient amounts of chromium, molybdenum, and nitrogen to produce a pitting resistance equivalent greater than 40. Duplex stainless steels have an attractive combination of mechanical and corrosion properties and are thus suitable for many marine and petrochemical applications, particularly where chlorides are present. The paper covers the following aspects of DSS: physical metallurgy, mechanical properties, corrosion properties, metallurgy of welding, machinability, and applications. A large number of references to the literature are given to aid the reader who is interested in acquiring a deeper understanding of the behaviour of this family of steels. *MST/1685*

 Manuscript received 11 May 1992. *The author is in the Research and Development Centre, AB Sandvik Steel, Sandviken, Sweden.*

Introduction

Duplex stainless steels (DSS) may be defined as a family of steels having a two phase ferritic–austenitic microstructure, the components of which are both stainless, i.e. contain more than 13%Cr*. In practice, the term DSS is reserved for alloys in which ferrite and austenite are present in relatively large separate volumes and in approximately equal volume fractions, as opposed to alloys in which one constituent appears in the form of small precipitates.

The discovery of a duplex microstructure was first described by Bain and Griffiths[1] in 1927 but it was not until the 1930s that DSS became commercially available. When the DSS were compared with austenitic steels several advantages became apparent, namely, higher mechanical strength, superior resistance to corrosion, and a lower price because of the low nickel content. It was later realised that advantages could be obtained from the use of DSS in environments where, owing to stress corrosion cracking, standard austenitic steels were inappropriate.[2,3] The interest in DSS in recent years derives from the high resistance of newly developed high alloy DSS to chloride induced corrosion, which is a problem of major concern in many marine and petrochemical applications. Perhaps even more important are the great improvements in weldability achieved by reducing the carbon content and increasing the nitrogen content.

An attractive combination of corrosion resistance and mechanical properties in the temperature range −50 to 250°C is offered by DSS. For example, the resistance to stress corrosion cracking and pitting corrosion is excellent and in many cases superior to that of standard austenitic steels of comparable cost.[4] Owing to the fine grained structure yield strength values typically twice those of austenitic grades are obtained in the annealed material state without any substantial loss in toughness. It is important to stress, however, that DSS are less suitable than austenitic steels above 250°C and below −50°C because of the brittle behaviour of ferrite at these temperatures. A factor of economic importance is the low content of expensive nickel, usually 4–7% compared with 10% or more in austenitic grades, as a result of which the life cycle cost of the DSS is the lowest in many applications.[5,6] Over the past decade there has been an increased use of nitrogen as an alloying element, stabilising austenite and therefore replacing nickel in this respect. As a result of this, austenite reformation during welding has become more rapid and in addition improved corrosion properties, in particular resistance to pitting corrosion, have been obtained.

Major review articles on DSS have been published by Solomon and Devine[7] in 1984 and more recently by Charles.[8] Although the present paper will be concerned with DSS in general, the emphasis will be placed on the super DSS, which have been developed to meet current requirements for pitting and stress corrosion resistance in chloride environments. These steels are defined as DSS having a pitting resistance equivalent (PRE) greater than 40, where[9,10]

$$\text{PRE} = \text{wt-\%Cr} + 3{\cdot}3(\text{wt-\%Mo}) + 16(\text{wt-\%N})$$

The present paper will be confined to wrought DSS, among which at least four different types can be identified:[8]

(i) low cost molybdenum free DSS of the type 23Cr–4Ni–0·1N: these steels provide alternatives to AISI 304 and 316
(ii) DSS of the type 22Cr–5Ni–3Mo–0·17N, the corrosion resistance of which lies between AISI 316 and 6%Mo + N superaustenitic grades
(iii) 25%Cr DSS with varying contents of molybdenum and nitrogen, sometimes with added copper and tungsten: the PRE values lie in the range 30–39
(iv) super DSS of the type 25Cr–7Ni–3·7Mo–0·27N having PRE values greater than 40.

A list of the most common wrought DSS that are commercially available is given in Table 1 together with tradename, producer, standard designation, and PRE value as defined according to the formula given above.

Structure of duplex stainless steels

PHASE EQUILIBRIA AT HIGH TEMPERATURES

There are many different ways of considering the Fe–Cr–Ni system. Pugh and Nisbet[11] used pseudobinary diagrams to describe the phase equilibria of DSS at elevated temperature whereas Colombier and Hochmann[12] used ternary sections. In the present study, a series of ternary sections for different temperatures was produced using the computer program Thermocalc developed by Sundman *et al.*[13] to calculate phase equilibria.

Figure 1 shows a sequence of isothermal ternary sections of the Fe–Cr–Ni–Mo–N system in the temperature range 1200–800°C. Whereas iron, chromium, and nickel were allowed to vary, a fixed content of 4%Mo and 0·3%N (typical of a super DSS) was assumed in these calculations. The compositions of the super DSS SAF 2507, UR 52N+,

*All compositions are in wt-%.

and Zeron 100 are represented roughly in these diagrams by the filled square. It should be pointed out that such diagrams can only be used qualitatively and can therefore only be used to show general behaviour. It is also worth commenting that these diagrams describe equilibrium conditions, which are rarely attained in practice. For example, whereas interstitial elements diffuse rather rapidly, the distribution of substitutional elements such as chromium, iron, nickel, and molybdenum remains virtually unchanged in practice during an annealing treatment in the range 1000–1100°C. This is particularly the case in austenite, in which diffusion rates are significantly lower than in ferrite.

All DSS solidify ferritically. The only phases that are thermodynamically stable for a 25Cr–7Ni super DSS in the range 1200–1000°C (Figs. 1*a*–1*c*) are ferrite (δ) and austenite (γ). These temperatures are representative of hot working, i.e. conditions under which the duplex structure is first established. At 900°C (Fig. 1*d*) Thermocalc predicts σ phase to be stable, whereas chromium nitrides of the type Cr_2N (ε) first become stable at somewhat lower temperatures as shown in Fig. 1*e*, calculated for 800°C. It is of interest to note that the intermetallic χ phase appears in the phase diagram at 800°C, thus confirming the experimental observation that the stability range of χ phase is significantly below that of σ phase. This will be discussed in more detail in the 'Precipitation of secondary phases' section below. Intermetallic R phase was also considered as a possible phase in the equilibrium calculations but did not appear as a stable phase at temperatures above 800°C.

STRUCTURE OF WROUGHT MATERIAL

The chemical composition and thermomechanical treatment of modern DSS are usually adjusted to give a volume fraction of ferrite of typically 40–45%. It is usual for DSS to be delivered in the annealed two phase condition, solution treatment usually being performed in the range 1050–1100°C. Hot working is performed typically in the temperature range 1000–1200°C, i.e. in the two phase regime of the isopleth diagram shown in Fig. 2. For super DSS hot working temperatures may be as high as 1300°C, at which temperature the structure is still duplex. Temperatures above this range may cause oxidation problems, whereas temperatures below 1000°C may result in precipitation and associated brittleness. Because of the small grain size, the DSS may become superplastic; advantage is sometimes taken of this effect during hot working.[14] The plastic deformation results in an elongation of the grains in the rolling direction and a development of texture, which often leads to rather strong anisotropy of the mechanical properties.[15] A typical microstructure of an extruded and cold pilgered tube of SAF 2507 is shown in Fig. 3, in which austenite appears in bright and ferrite in dark contrast. This structure, which is typical of a DSS in its as delivered condition, is entirely duplex and no precipitated secondary phases are present.

PRECIPITATION OF SECONDARY PHASES

In addition to ferrite (δ) and austenite (γ) a large variety of undesirable secondary phases may form in the temperature range 300–1000°C in DSS during isothermal aging or incorrect heat treatment. This is essentially a consequence of the instability of ferrite. The following phases have been observed: σ phase, Cr_2N, CrN, secondary austenite, χ phase, R phase, π phase, M_7C_3, $M_{23}C_6$, Cu, and τ phase. Moreover, in the range 300–500°C, spinodal decomposition of ferrite can occur. Of the phases listed above, σ phase is by far the most important because of its influence on toughness and corrosion behaviour. A summary of these phases is given in Table 2, together with information on corresponding temperature range of precipitation, lattice parameter, crystal structure, and original reference.

σ PHASE

It is well known that σ phase is formed in a large number of DSS.[24–27] This situation is accentuated in all super DSS by the increased amount of chromium and molybdenum relative to conventional DSS, as a result of which the 'C' curves of σ phase (as well as other intermetallic phases) are displaced towards shorter times.[8] Molybdenum is also known to increase the range of stability of σ phase towards high temperatures. In addition to the effects of chromium and molybdenum it is of interest to investigate to what extent tungsten and copper, which are sometimes used as alloying elements in DSS, influence the precipitation behaviour. Careful experiments on the precipitation kinetics in super DSS of various compositions performed by Charles[8] show that tungsten, like molybdenum, increases the precipitation rate of σ phase and expands the corresponding C curve towards higher temperatures. In contrast, no effect of copper was observed in this respect.[8] All the above effects must be taken into consideration during production since σ phase adversely affects both hot ductility[28] and room temperature ductility.[24] Precipitation of σ phase often occurs at triple junctions or at ferrite/austenite phase boundaries; an example is presented in Fig. 4, which shows the microstructure of SAF 2507 after isothermal aging at 850°C.

Table 1 Chemical composition (wt-%) of most common wrought duplex stainless steels

Tradename	Producer	Standard	Cr	Mo	Ni	N	Other elements	PRE
SAF 2304	Sandvik, Avesta*	UNS S 32304	23	0·2	4	0·1	...	25
UR 35N	Creusot-Loire	UNS S 32304	23	0·2	4	0·1	...	25
3RE60	Sandvik, Avesta	UNS S 31500	18·5	2·7	5	0·07	1·5Si	29
UR 45N	Creusot-Loire	UNS S 31803	22	3	5·3	0·17	...	35
SAF 2205	Sandvik	UNS S 31803	22	3	5·3	0·17	...	35
2205	Avesta	UNS S 31803	22	3	5·3	0·17	...	35
FALC 223	Krupp Stahl	UNS S 31803	22	3	5·3	0·17	...	35
AF 22	Mannesmann	UNS S 31803	22	3	5·3	0·17	...	35
VS 22	Valinox	UNS S 31803	22	3	5·3	0·17	...	35
10RE51	Sandvik	UNS S 32900	25	1·5	4·5	...	...	30
DP 3	Sumitomo	UNS S 31260	25	3	6·5	0·16	0·5Cu, 0·3W	37
UR 52N	Creusot-Loire	UNS S 32550	25	3	6·5	0·18	1·6Cu	38
Ferralium 255	Langley Alloys	UNS S 32550	25	3	6·5	0·18	1·6Cu	38
UR 47N	Creusot-Loire	UNS S 32200	25	3	6·5	0·18	...	38
Zeron 100	Weir	UNS S 32760	25	3·6	7	0·25	0·7Cu, 0·7W	41
UR 52N+	Creusot-Loire	UNS S 32550	25	3·8	6	0·26	1·5Cu	42
SAF 2507	Sandvik, Avesta*	UNS S 32750	25	3·8	7	0·27	...	42

PRE pitting resistance equivalent.
*Under licence from AB Sandvik Steel.

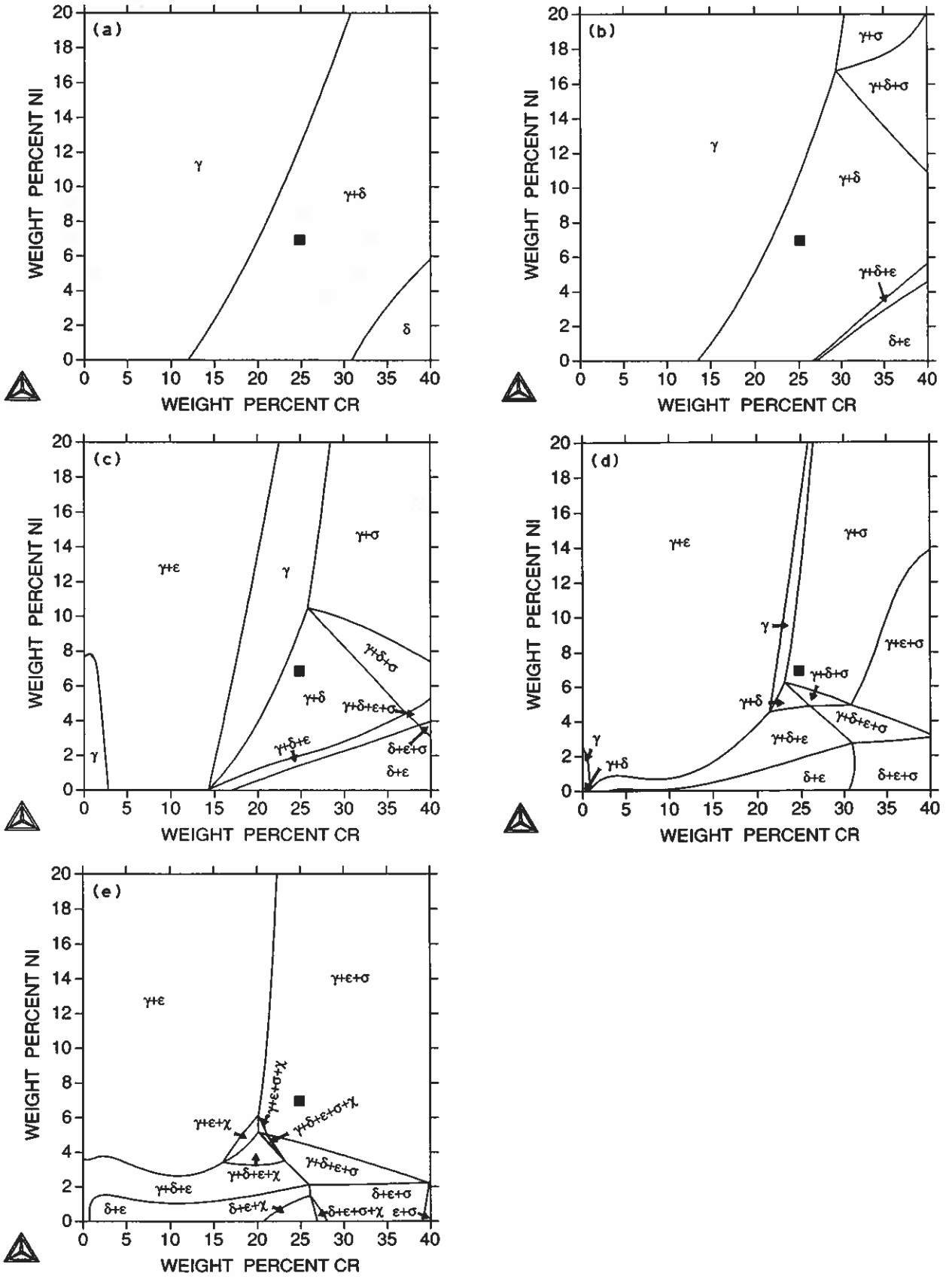

1 Isothermal sections of Fe–Cr–Ni–Mo–N system at *a* 1200, *b* 1100, *c* 1000, *d* 900, and *e* 800°C calculated using Thermocalc computer program for fixed fractions of 4%Mo and 0·3%N: composition of super duplex stainless steel (DSS) is indicated by filled square

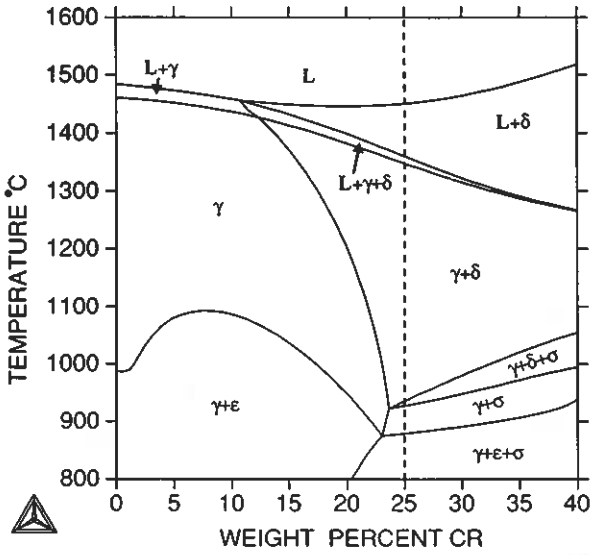

2 Computer calculated isopleth diagram above 800°C: dotted line corresponds to composition of super DSS

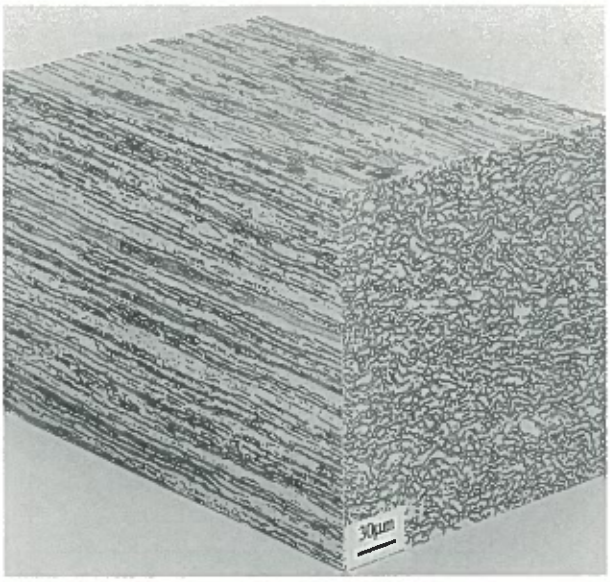

3 Typical microstructure of seamless tube of SAF 2507 in annealed condition, showing elongation of grains in rolling direction (optical)

Quantitative chemical analysis shows that chromium, molybdenum, and silicon are enriched in σ phase.[27] It is also of interest to note that chromium and molybdenum increase both the precipitation rate and the volume fraction of σ phase in a large number of duplex steels. Since super DSS are rich in these elements, they are inherently more sensitive than conventional DSS and therefore require faster cooling.[30] Maehara *et al.*[27] also found that nickel accelerated the precipitation kinetics of σ phase, although the equilibrium volume fraction was reduced.

This paradox can be understood in terms of the associated reduced ferrite fraction, which leads to a partitioning of σ promoting elements, such as chromium and molybdenum, to the ferrite. A factor which must be considered in hot working is that deformation enhances σ phase formation. Laboratory experiments have shown that plastic deformation in the range 800–900°C can reduce the time required to form σ phase by one order of magnitude.[31]

An important observation is that the precipitation behaviour of σ can be influenced to a large extent by altering the heat treatment. A high solution treatment temperature tends to increase the volume fraction of ferrite which will consequently be diluted with respect to ferrite forming elements. This will of course also suppress the σ phase formation as has been verified experimentally in a super DSS.[30] The time delay can in extreme cases be as large as a factor of five.[31] The cooling rate is also a vital factor. Theoretical and experimental investigations of SAF 2507 have shown that the critical cooling rate to form 1% σ phase is 0·4 K s^{-1} when a solution temperature of 1060°C is used. The computer program developed by Josefsson *et al.*[30] allows such estimations to be made in any DSS provided the time–temperature–transformation (TTT) diagram has been established.

Whereas σ phase is avoided by cooling from a high solution temperature, the conditions for Cr_2N precipitation will become more favourable, a factor that complicates heat treatment for nitrogen alloyed DSS. This will be discussed in the following subsection.

CHROMIUM NITRIDES

With the increased use of nitrogen as an alloying element in DSS, and in super DSS in particular, the precipitation of Cr_2N in the temperature range 700–900°C has become more important.[32] The formation of Cr_2N is likely to occur when rapid cooling takes place from a high solution temperature because supersaturation of nitrogen in ferrite will occur as a consequence. In such cases elongated Cr_2N particles often precipitate intragranularly with the crystallographic relation $\langle 0001\rangle_{Cr_2N} \| \langle 011\rangle_{\delta}$, an example of which is shown in Fig. 5. Isothermal heat treatment in the range 700–900°C usually results in the precipitation of intergranular Cr_2N, which decorates either δ/δ grain boundaries or γ/δ phase boundaries. An example of Cr_2N precipitating at γ/δ phase boundaries on aging at 850°C

Table 2 Phases observed in duplex stainless steels

Type of precipitate	Nominal chemical formula	Temperature range in DSS, °C	Space group	Lattice parameter, nm	Ref.
Ferrite (δ)	...	...	$Im3m$	a = 0·286–0·288	...
Austenite (γ)	...	...	$Fm3m$	a = 0·358–0·362	...
σ	Fe–Cr–Mo	600–1000	$P4_2/mnm$	a = 0·879, c = 0·454	16
Chromium nitride	Cr_2N	700–900	$P31m$	a = 0·480, c = 0·447	17
Chromium nitride	CrN	...	$Fm3m$	a = 0·413–0·447	...
χ	$Fe_{36}Cr_{12}Mo_{10}$	700–900	$I43m$	a = 0·892	18
R	Fe–Cr–Mo	550–650	$R3$	a = 1·090, c = 1·934	19
π	$Fe_7Mo_{13}N_4$	550–600	$P4_132$	a = 0·647	20
τ	ND	550–650	$Fmmm$	a = 0·405, b = 0·484, c = 0·286	21
M_7C_3	...	950–1050	$Pnma$	a = 0·452, b = 0·699, c = 1·211	22
$M_{23}C_6$	...	600–950	$Fm3m$	a = 1·056–1·065	23

ND not determined.

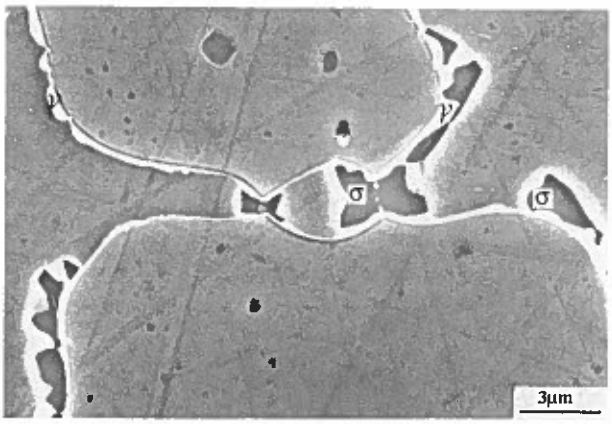

4 Microstructure of SAF 2507 aged for 10 min at 850°C, showing σ phase at ferrite/ferrite phase boundaries and austenite/ferrite boundaries: secondary austenite is visible in bright contrast between primary austenite and ferrite[29] (SEM)

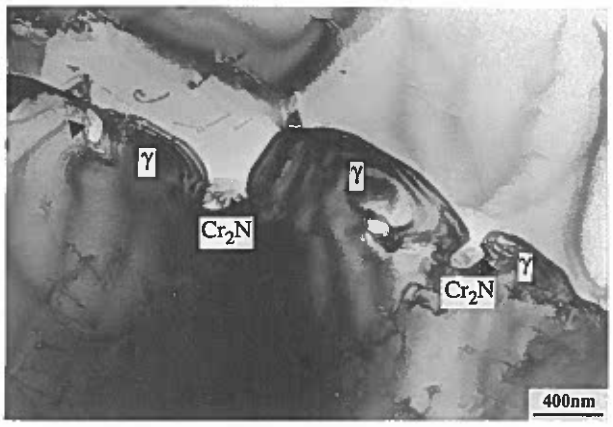

6 Intergranular Cr_2N and secondary austenite formed in SAF 2507 after aging for 10 min at 850°C (TEM): Cr_2N particles can be observed to exert pinning force on migrating austenite/ferrite boundary[29]

for 10 min is shown in Fig. 6, in which simultaneous precipitation of secondary austenite is also demonstrated. The Cr_2N formed under these conditions has an influence on pitting corrosion, which will be discussed further in the 'Corrosion' section below.

Whereas hexagonal Cr_2N appears to be the predominating type of nitride, cubic CrN has been observed by Hertzman *et al.*[33] in the heat affected zone of welds of SAF 2205. However, they observed little or no adverse effect on toughness and corrosion properties. This seems to be the only reported observation of CrN in DSS.

SECONDARY AUSTENITE

Decomposition of ferrite to austenite can occur over a wide temperature range.[24,31] This can be understood on the basis that the duplex structure is quenched from a higher temperature, at which the equilibrium fraction of δ is higher. There appear to be three mechanisms (in addition to the direct transformation of ferrite to austenite occurring at very high temperatures) by which austenite can precipitate in δ ferrite:

(i) by the eutectoid reaction $\delta \rightarrow \sigma + \gamma$
(ii) as Widmannstätten precipitates
(iii) via a martensitic shear process.

The eutectoid reaction is facilitated by the rapid diffusion along δ/γ boundaries and often results in a typical eutectoid structure of σ phase and austenite in prior ferrite grains (*see* Fig. 7). This typically occurs in the temperature range 700–900°C, in which δ is destabilised by the precipitation of σ phase, reducing the chromium and molybdenum content in the ferrite.

Southwick and Honeycombe[34] found that below about 650°C, ferrite in an experimental DSS transformed to austenite via a mechanism that showed great similarities with martensite formation. This austenite precipitated isothermally and showed no difference in composition compared with the ferritic host lattice, thus indicating that the transformation was diffusionless with respect to substitutional elements. The orientation relationship was found to obey the Nishiyama–Wasserman relation.

At temperatures above 650°C, at which diffusion is more rapid, austenite formed as Widmannstätten precipitates having various morphologies.[34] This austenite obeyed the usual Kurdjumov–Sachs relationship and also showed a significantly higher nickel content than the surrounding ferrite, indicating that the transformation was diffusion assisted. This was also indirectly confirmed since C curve kinetics was observed.

The secondary austenite formed at δ/γ phase boundaries has been found to be poor in chromium, particularly when Cr_2N precipitates cooperatively. This explains why pitting attack can occur in these areas and also shows that pitting is sometimes a problem although the amount of σ phase is considered to be negligible.[29]

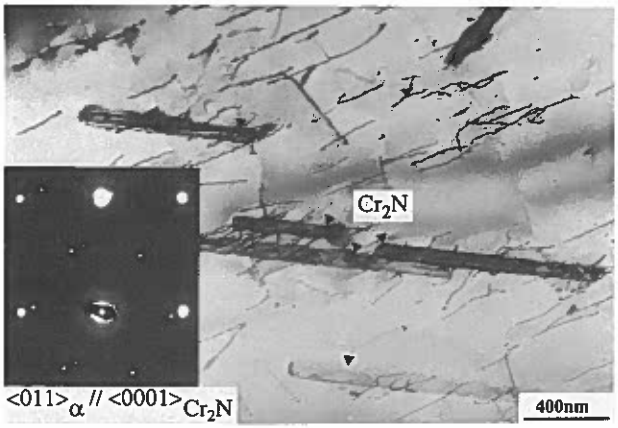

5 Intragranular Cr_2N formed in SAF 2507 after aging for 10 min at 850°C (TEM): as shown by inset, orientation relationship with matrix is $\langle 0001 \rangle_{Cr_2N} \| \langle 011 \rangle_\delta$ (From Ref. 29)

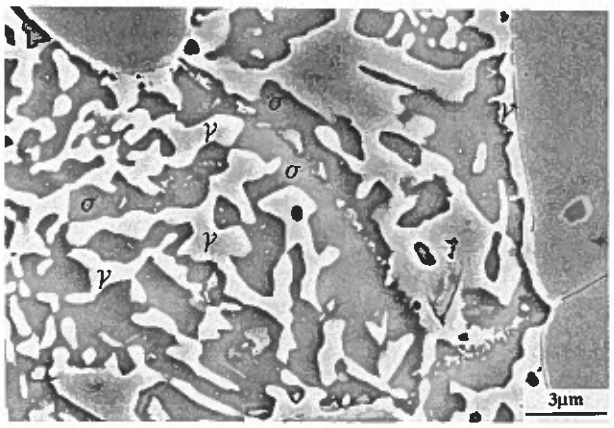

7 SEM of SAF 2507 aged for 72 h at 700°C, showing decomposition of ferrite into eutectoid structure of σ phase and secondary austenite[29]

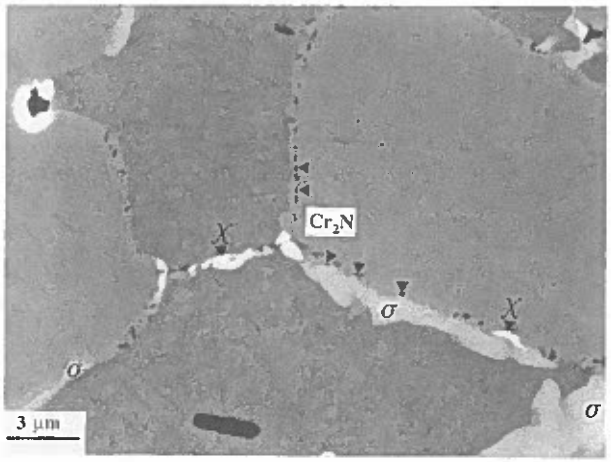

8 Backscattered SEM of polished surface of SAF 2507 aged for 10 min at 850°C, showing atomic number contrast: particles in bright contrast are χ phase, and σ phase appears in darker contrast

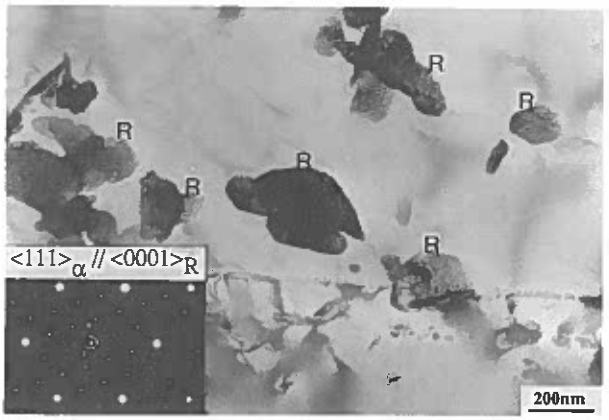

9 TEM of 22Cr–8Ni–3Mo weld metal aged for 24 h at 600°C, showing *R* phase precipitates with uneven contrast in ferrite grain: as shown by inset, orientation relationship is $\langle 0001\rangle_R \| \langle 111\rangle_\delta$ (From Ref. 35)

χ PHASE

Although intermetallic χ phase is commonly found in DSS in the temperature range 700–900°C, it is usually present in much smaller quantities than σ phase. The 'nose' of the C curve usually appears at lower temperatures than for σ phase. For instance, in SAF 2507 this temperature was 850°C, which is about 75°C lower than that for σ phase in the same alloy.[29] The χ phase has an adverse effect on toughness and corrosion properties but its effect is often difficult to separate from that of σ phase since χ phase and σ phase often coexist. Owing to the lower volume fraction of χ phase it is less important than σ phase, but its effect cannot always be ignored. For example, below the C curve of σ phase in SAF 2507, pitting temperatures can be low although there is virtually no σ phase. Precipitation of χ phase is in part responsible for this, because it consumes chromium and molybdenum and the simultaneously formed secondary austenite becomes poor in these elements.[29]

The χ phase can of course be identified using electron diffraction in the analytical transmission electron microscope (TEM). However, a much more useful survey of the distribution of χ phase is obtained when a plane specimen is imaged in the scanning electron microscope (SEM) using backscattered electrons. Owing to the higher content of molybdenum, often about 20% (Ref. 35), in combination with the large atomic scattering factor of molybdenum, χ phase appears in brighter contrast than σ phase. This is distinctly demonstrated in Fig. 8.

R PHASE

Since the observation of *R* phase was reported by Hochmann *et al.*,[36] *R* phase has been found to precipitate in DSS in the range 550–700°C. The *R* phase is a molybdenum rich intermetallic compound having a trigonal crystal structure. In a recent investigation of 22Cr–8Ni–3Mo weld metal the *R* phase was found to have an approximate composition of 30%Fe, 25%Cr, 6%Ni, 35%Mo, and 4%Si.[35] An uneven contrast is often shown by *R* phase in the TEM, an example of which is shown in Fig. 9, although this criterion alone is not sufficient for identification but must be complemented with electron diffraction analysis (*see* Fig. 9 inset). It was also found in this investigation[35] that toughness and critical pitting temperature were reduced by the formation of *R* phase. Both intergranular and intragranular precipitates have been observed. The intergranular precipitates are perhaps even more deleterious as regards pitting corrosion as they may contain as much as 40%Mo.[35] Since *R* phase is observed in SAF 2507 (Ref. 29) it can also be expected to be found in other super DSS.

π PHASE

An observation of interest is the recent discovery of the nitride π phase in the duplex weld metal 22Cr–8Ni–3Mo.[35] This phase was found within the grains and, like *R* phase, contributed to embrittlement and pitting corrosion in material aged isothermally at 600°C. The π phase was found to contain approximately 28%Fe, 35%Cr, 3%Ni, and 34%Mo, thus showing that the ideal chemical formula proposed ($Fe_7Mo_{13}N_4$) is only a rough approximation. In contrast to *R* phase, π phase has a cubic crystal structure and shows an even contrast in the TEM (*see* Fig. 10).

CARBIDES

In relatively carbon rich DSS, carbides of the type M_7C_3 precipitate in the range 950–1050°C, whereas $M_{23}C_6$ carbides precipitate below 950°C. Both types of carbide are observed predominantly at δ/γ phase boundaries,[37] but precipitation at δ/δ and γ/γ boundaries has also been observed.[38] Carbides play a less important role in super DSS than in traditional DSS because of the low carbon content, which is often in the range 0·010–0·020%. Indeed,

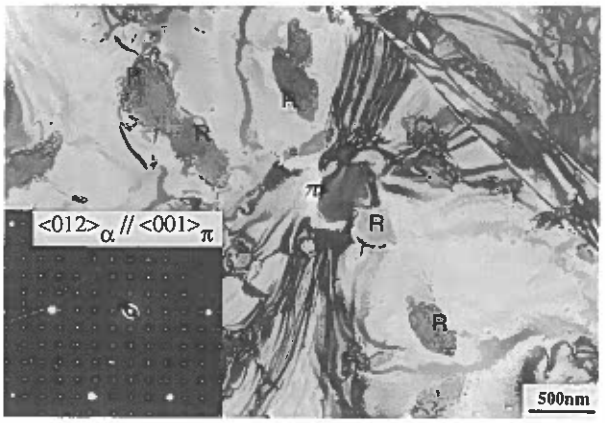

10 TEM of 22Cr–8Ni–3Mo weld metal aged for 24 h at 600°C, showing π phase precipitates with even contrast in ferrite grain: as shown by inset, orientation relationship is $\langle 001\rangle_\pi \| \langle 012\rangle_\delta$ (From Ref. 35)

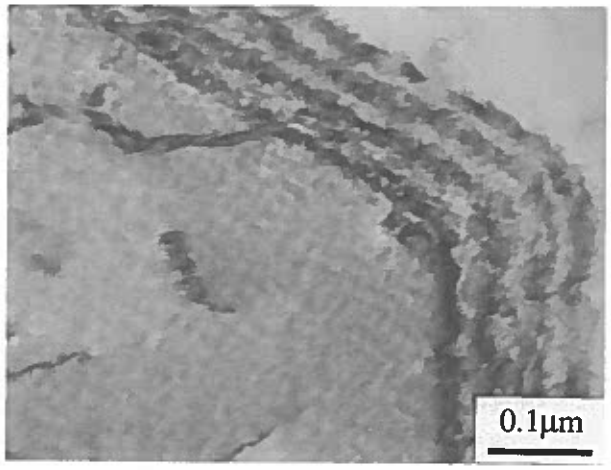

11 TEM of 22Cr–8Ni–3Mo weld metal aged for 24 h at 500°C: modulated contrast typical of spinodal decomposition is visible in ferrite grain to left[35]

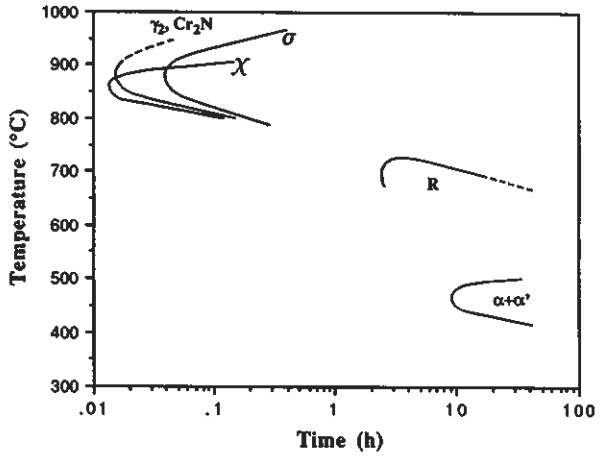

12 Temperature–time–precipitation curves for various precipitates observed in SAF 2507

although thoroughly investigated, SAF 2507 shows no precipitation of carbides of any type. This implies that classical intergranular corrosion similar to that in austenitic steels, caused by carbide precipitation and associated chromium depletion at grain boundaries, is unlikely to occur in modern DSS.

PRECIPITATION OF LESS COMMON PHASES

Copper particles have been observed in copper rich DSS. However, some of these observations are somewhat ambiguous since, as was pointed out by Solomon and Devine,[7] copper and austenite are both fcc and exhibit the Kurdjumov–Sachs relationship. Direct observation of copper particles in a 3%Cu DSS was made by Soylu and Honeycombe[39] using energy dispersive X-ray analysis of thin foil specimens in an analytical TEM. They found that the copper particles promoted nucleation of austenite, with a concomitant refinement in microstructure. Copper rich precipitates have also been observed in copper bearing super DSS.[8]

Another unusual phase in DSS is the τ phase, which was recently discovered in an alloy of the type 22Cr–5Ni–3Mo.[21] However, its effect on the materials properties was not investigated.

475°C EMBRITTLEMENT

This type of embrittlement has been observed to occur in ferritic steels[40,41] and in DSS[42–47] at temperatures below about 500°C. This is a consequence of the miscibility gap in the Fe–Cr system as proposed by Williams.[48] The embrittling reaction can be of two fundamentally different types; inside the spinodal in the equilibrium diagram spinodal decomposition of ferrite into chromium rich α' and iron rich α occurs, whereas outside the spinodal but still within the miscibility gap classical nucleation and growth of α' occurs.[49,50] Irrespective of the reaction by which it is formed, α' results in an embrittlement of the ferrite and an associated increase in hardness. Although the embrittlement rate is faster at higher temperatures the phenomenon has been observed at temperatures as low as 280°C in welds of 22Cr–5Ni steel held for times greater than ~1000 h (Ref. 42).

Chromium, molybdenum,[47] and copper[8] have been found to promote 475°C embrittlement. This must be taken into consideration in the use and production of super DSS that are rich in these elements. Nickel also has an effect on spinodal decomposition but, in contrast to chromium and molybdenum, the effect is of an indirect nature since nickel promotes partitioning of chromium and molybdenum to the ferrite. Spinodal decomposition in ferritic steels is enhanced by the presence of nitrogen.[51] However, the situation in DSS is more complex since nitrogen is partitioned to austenite and therefore the amount of nitrogen dissolved in ferrite is not a simple function of the average nitrogen content.

Although hardness and toughness are the most sensitive of the parameters that can be used to identify 475°C embrittlement, it can also be revealed as a modulated contrast of ferrite. The distinctive contrast becomes visible in the TEM in the overaged condition when the ferrite crystal is perfectly aligned on zone axis ⟨001⟩; an example is shown in Fig. 11. In this image the absence of grain boundary zones denuded of particles is apparent, an observation that is often interpreted as a sign of absence of nucleation, which is characteristic of spinodal decomposition.

Enhanced hardening and associated embrittlement owing to the presence of copper and tungsten have been observed recently in DSS below about 500°C (Ref. 8). The mechanism seems to be different from the classical 475°C embrittlement described above since it involves nucleation of copper rich precipitates. However, the phenomenon must be taken into consideration in copper and tungsten bearing DSS.

TTT DIAGRAM FOR SUPER DSS

The results in this section can be summarised in a TTT diagram showing the C curves for the most common precipitates in SAF 2507 solution treated at 1060°C. This diagram, shown in Fig. 12, is a synthesis of recent results obtained above 700°C by Nilsson *et al.*[29] and below 700°C by Wilson[52] from a combined use of hardness measurements, SEM analysis, and X-ray analysis of extracted residue. A notable feature is the absence of carbides. It is also worth mentioning that χ phase is observed at somewhat lower temperatures and shorter times than σ phase. The shape of the C curve for R phase is intended to indicate that this phase appears to be unstable after long aging times.

Mechanical properties

TENSILE STRENGTH

The strength in the quench annealed condition of the most common types of DSS is compared with that of fully austenitic and ferritic alloys in Table 3. It can be seen that the yield strength of DSS is between two and three times that of the austenitic grade AISI 304.

For the same interstitial content ferrite is usually stronger than austenite but less ductile. Since the DSS contain both ferrite and austenite they may perhaps be expected to have properties determined by a linear law of mixtures. This is approximately correct regarding elongation but the situation as regards tensile strength is more complex since it depends strongly on grain size, which is usually smaller in DSS. Floreen and Hayden[53,54] investigated DSS of varying compositions starting from a nominal composition of 25Cr–6Ni. A series of tieline alloys ranging from 100% ferrite to 100% austenite was produced and investigated mechanically. When the effect of grain size was compensated for these authors could conclude that the strength of the basic 60% ferrite/40% austenite alloy was controlled essentially by the stronger ferritic component. However, owing to the smaller grains in the duplex alloy, there was a considerable grain size contribution to the strength as described by the well known Hall–Petch relation.[55] This implied that in practice the duplex alloy achieved a higher strength than its constituents. This phenomenon is also reflected in the present investigation as a yield stress that is significantly higher for all DSS than for the ferritic and austenitic grades (*see* Table 3).

In the examples given above austenite is weaker than ferrite but this need not necessarily be the case in a duplex alloy. For example, in nitrogen alloyed DSS, nitrogen is partitioned to austenite to such an extent that the austenitic phase may become stronger than the ferritic phase. Wahlberg[43] found a higher microhardness in the austenite grains in a 0·20%N type 22Cr–5Ni steel for which an equilibrium concentration of 0·38% nitrogen in austenite is predicted by Thermocalc.[13] In super DSS additional strengthening is caused by solid solution hardening by the substitutional elements chromium and molybdenum, and by the interstitial element nitrogen. For example, in super DSS containing 0·27%N the amount of dissolved nitrogen in the austenite can be as high as 0·45% (Ref. 8). Since the grain sizes are similar for the DSS in Table 3 it can be concluded that the increase in strength with increased additions of alloying elements reflects the solid solution strengthening effects of chromium, molybdenum, and nitrogen.

TOUGHNESS

Annealed condition

Whereas the tensile properties of DSS were found to be governed essentially by the ferrite phase, Floreen and Hayden[53] concluded that the good toughness could be ascribed to the presence of austenite. They concluded that cleavage fracture of ferrite was retarded by the more ductile austenite. However, as can be seen in Table 3, the toughness of quench annealed material decreases somewhat with increasing alloying additions although the value of 230 J for the super DSS may still be regarded as very high. It should also be pointed out that the transition from ductile to brittle fracture for DSS in the annealed material state occurs at −60°C or below,[8] which is quite satisfactory for most applications considered.

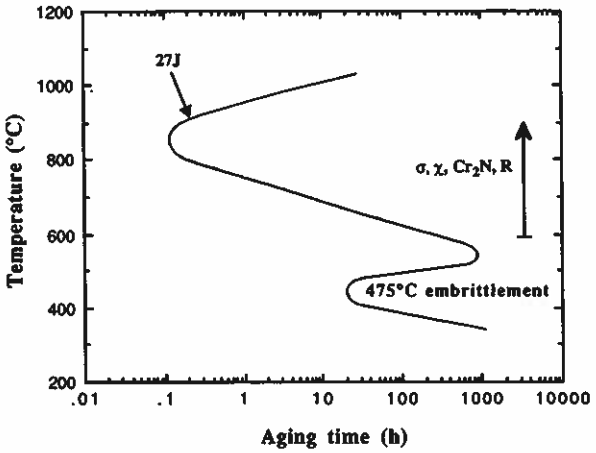

13 Time–temperature–transformation (TTT) diagram for SAF 2507, with curve corresponding to 27 J impact toughness indicating rate of embrittlement at various temperatures

Because DSS often exhibit texture, particularly in the cold rolled condition, a strong anisotropy of mechanical properties can be expected. In cold rolled sheet of 22Cr–5Ni–3Mo steel the texture was found to be (100)[001] in ferrite and {110}⟨112⟩ in austenite.[15] This has been shown to lead to values of impact toughness[56] and fracture toughness[57] that are higher in the transverse than in the longitudinal direction relative to the banded structure.

Influence of precipitates

The above discussion has been confined to the influence of ferrite and austenite and the influence of secondary particles has not been taken into consideration. As discussed in the 'Precipitation of secondary phases' section above, decomposition of ferrite becomes important at temperatures above about 300°C and a large number of embrittling phase transformations may occur. This was investigated by Hochmann *et al.*[32] There are two temperature ranges in which embrittlement occurs; in the range 600–900°C the impact toughness is reduced essentially by σ phase, whereas 475°C embrittlement may cause brittleness below about 500°C. Between 500 and 600°C some embrittlement occurs, although in this range the precipitation reactions are significantly slower. This is reflected as a 'bay' in the isothermal transformation diagram of super DSS as shown in Fig. 13, where critical toughness levels are reached after about 10 h of isothermal aging,[52,24,35] the exact time being dependent upon chemical composition and prior solution heat treatment. Although σ phase appears to be the most deleterious phase owing to its large volume fraction, it should be pointed out that other phases such as Cr_2N, χ, R, and π may contribute to

Table 3 Typical values of mechanical properties of austenitic and ferritic stainless steels and solution annealed DSS: values given should be used for comparison only

Alloy	Standard	0·2% proof stress (min.), MN m^{-2}	Ultimate tensile strength, MN m^{-2}	Elongation (min.) A5, %	Impact toughness at RT, J	Fluctuating tension fatigue strength, MN m^{-2}
AISI 304	UNS S 30400	210	515–690	45	>300	120 ± 120
AISI 430	UNS S 43000	205	450	20	...	...
23Cr–4Ni (SAF 2304)	UNS S 32304	400	600–820	25	300	245 ± 245
22Cr–5Ni–3Mo (SAF 2205)	UNS S 31803	450	680–880	25	250	285 ± 285
25Cr–7Ni–4Mo (SAF 2507)	UNS S 32750	550	800–1000	25	230	300 ± 300

RT room temperature.

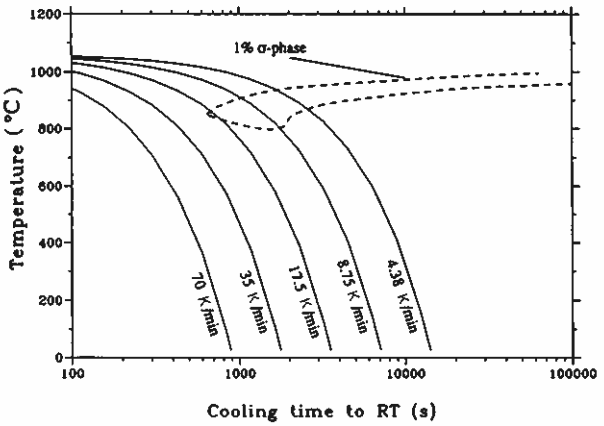

14 Calculated continuous cooling transformation (CCT) diagram of SAF 2507 based on experimentally obtained TTT diagram[30]

brittle behaviour above 600°C. Since these phases often coexist it is difficult to separate their relative contributions. In a recent investigation of a super DSS, however, aging at 800°C for 10 min, causing precipitation of χ phase and Cr_2N at grain boundaries but virtually no σ phase, resulted in an impact value of about 80 J (Ref. 29). This shows that in the absence of σ phase, Cr_2N and χ phase may be as detrimental to toughness. Typically, *R* phase and π phase precipitate at about 600°C, and have been shown to reduce toughness in 22Cr–8Ni–3Mo welds.[35] An important implication of this is that cooling from solution heat treatment must be sufficiently rapid to avoid these precipitates. A computer program to estimate the critical cooling rate from isothermal diagrams has been developed.[30] For example, in SAF 2507 solutionised at 1060°C, the critical cooling rate to form 1% σ phase was found to be 0·4 K s^{-1} (*see* Fig. 14). It should be mentioned in this context that DSS usually tolerate as much as 4% σ phase before the critical impact energy of 27 J is reached.[29] However, such a microstructure can of course not be tolerated because of the low corrosion resistance.

The occurrence of 475°C embrittlement in DSS can be caused by true spinodal decomposition of ferrite or by classical nucleation and growth of α'. Although this usually takes place below 500°C, α' precipitation has been shown to occur at temperatures as high as 600°C in the DSS U50 (Ref. 58). Regardless of the mechanism of 475°C embrittlement, reduced toughness is an inevitable consequence.[24,35,42] It is important to mention that low temperature embrittlement can occur even at temperatures <300°C, albeit after very long aging times. For example, in SAF 2205 embrittlement was observed after about 1000 h aging at 280°C (Ref. 42). As a consequence, there are fundamental limits on the temperature range within which DSS can be employed. The maximum recommended temperature is very much dependent on chemical composition and type of application. For SAF 2205 the critical time to reach 27 J impact energy has been estimated to be 20 years at 310°C (Ref. 59). As shown by Hertzman,[42] a difference in aging response can also be expected between virgin material and welds, presumably because of the stresses generated during the welding operation in combination with strong partitioning of chromium and molybdenum to the ferrite.

FATIGUE STRENGTH

Owing to the higher strength of DSS compared with austenitic steels the former are more resistant to fatigue. Furthermore, provided corrosion mechanisms can be ignored, they show a rather well defined fatigue limit when

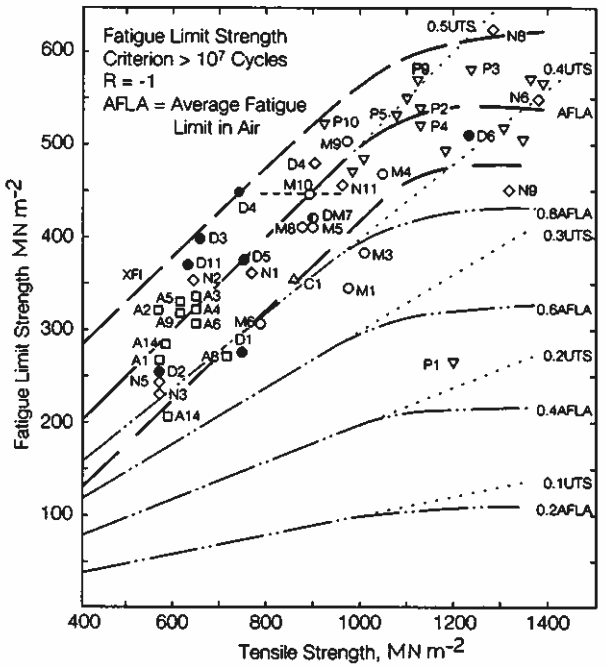

15 Unnotched rotating bending fatigue limits versus tensile strength for various types of stainless steel (From Ref. 66)

tested in stress controlled fatigue. This was demonstrated during testing in an air environment in a 22Cr–5Ni–3Mo steel by Mathis,[60] and in a 26Cr–6Ni–4Mo steel by Atrens.[61] A well defined fatigue limit was also observed by Magnin *et al.* in a 21Cr–7Ni steel.[62] Typical values of the fatigue limit in fluctuating tension are given in Table 3, from which it can be seen that the fatigue strength of DSS is directly related to the yield strength.[63] This can be understood on the basis that, in the examples given above, the maximum stress in each fatigue cycle will be approximately equal to the yield stress. At this stress level plastic deformation is sufficient to cause initiation of small fatigue cracks at inclusions, persistent slip bands, or phase boundaries.[64] In an investigation of DSS tieline alloys ranging from pure austenite to pure ferrite, Hayden and Floreen[65] found that the DSS were superior to the single phase alloys and attributed this essentially to the effect of the fine grain size of the duplex structure.

As shown by Haynes[66] the fatigue properties are improved with increased static strength, i.e. with cold work, up to a tensile strength of about 1000 MN m^{-2}, above which a plateau is reached. The results can be observed in Fig. 15. The fatigue properties can also be expected to be strongly dependent upon the orientation of the stress axis because of the texture.

CORROSION FATIGUE

Under corrosive conditions the fatigue strength is reduced and a true fatigue limit is no longer observed.[60–62] The interaction between fatigue and corrosion is very complex but there seems to be a strong correlation between pitting resistance and corrosion fatigue resistance, presumably because corrosion pits provide initiation sites for fatigue cracks.[67] When comparing fatigue data for different types of DSS Charles[8] found that alloys having higher PRE values were more resistant to corrosion fatigue. Under conditions where no pitting was expected the fatigue strength in seawater environments was found to be comparable to the fatigue behaviour in air. Some caution must be used when interpreting such data, however, since the corrosion fatigue behaviour depends strongly on the

type of environment, test frequency, and potential.[68] For example, enhanced crack growth rates involving cleavage fracture of the ferrite can be observed when hydrogen is present, as reported in a recent investigation of Zeron 100 (Ref. 69). Therefore, when the fatigue life of a component is to be estimated, it is essential that the tests be performed in environments that are relevant to the actual application.

Corrosion

Although DSS have attractive mechanical properties, it is largely because of their corrosion properties, e.g. pitting corrosion, stress corrosion, and intergranular corrosion, that they have received so much attention. The behaviour of DSS is in many corrosive environments comparable or superior to that of austenitic steels containing comparable additions of chromium and molybdenum. The emphasis in this section will be placed mainly on the major types of corrosion, namely, localised (pitting) corrosion and stress corrosion cracking, whereas intergranular corrosion, which is a minor problem in DSS, will be discussed only briefly. Pitting corrosion is perhaps the most harmful of these since corrosion pits often provide initiation sites for fatigue cracks and stress corrosion cracks.

The subject of corrosion is enormous and very complex and therefore virtually impossible to cover in a general overview of this nature. For example, the relative positions of alloys in corrosion tests are found to be strongly dependent on the environment. The reader who is interested in gaining a deeper understanding of this subject is directed to the review articles on corrosion in DSS that are available[4,7,70] and to the reference lists presented in these.

LOCALISED CORROSION

The resistance to localised corrosion in steels is strongly dependent on the chemical composition. Generally, DSS are at least as resistant as austenitic steels of the same chromium and molybdenum content. In practice, partly because of the alloying additions of nitrogen in many modern DSS, the resistance is often much higher, particularly in chloride containing environments. It is well known that chromium, molybdenum, and nitrogen improve the resistance to pitting corrosion in Fe–Ni–Cr alloys. The effect of these elements can be quantified by an empirical parameter termed pitting resistance equivalent (PRE) which is defined generally as follows[9,10,71]

$$\mathrm{PRE} = \%\mathrm{Cr} + 3{\cdot}3(\%\mathrm{Mo}) + k(\%\mathrm{N})$$

where k is a number between 10 and 30, the value 16 being most frequently used. Although this parameter has some limitations because it only includes the effect of three elements, it offers a useful and quick way of estimating pitting resistance. A more complete description of the influence of different elements on pitting and crevice corrosion is given elsewhere.[4] The usefulness of the PRE can be appreciated with reference to Fig. 16, which shows the relation between PRE and the critical pitting temperature (CPT) for a number of different steels. It is worth commenting that the linear relation obtained in Fig. 16 for both austenitic steels and DSS illustrates the well known characteristic that localised corrosion is almost insensitive to ferrite/austenite ratio and is essentially governed by the chemical composition. In spite of some scatter of data points such diagrams can be used for ranking of alloys. The super DSS and the superaustenitic steels,[72,73] which have PRE values above 40, can be found to have CPT values as high as 80°C using the modified ASTM G48 test.[74] It must be pointed out that these results were obtained on solution treated laboratory material in its ideal condition. Therefore, CPT values of 80°C cannot be guaranteed for commercial material taken from the production line.

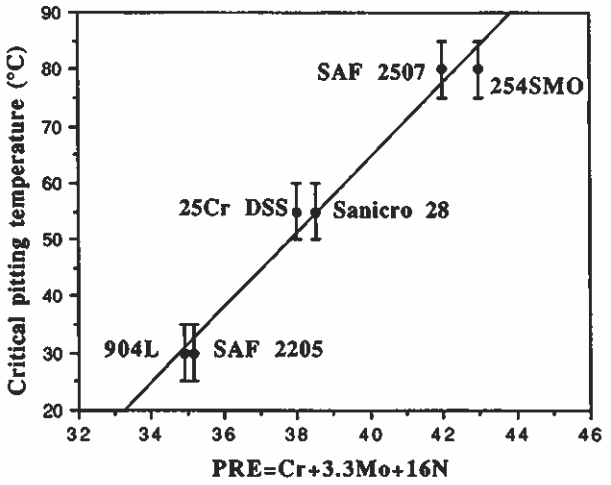

16 Relation between PRE value and critical pitting temperature for most common DSS grades and three austenitic steel grades

Although the formula given above describes the influence of chromium, molybdenum, and nitrogen in detail it is unable to take into consideration effects of microstructural inhomogeneities. First, if differences in PRE between austenite and ferrite in a DSS exist this will cause preferential attack of the weakest phase. In SAF 2507 the pitting resistance has been optimised by performing the solution treatment at a temperature at which thermodynamic equilibrium between the two phases leads to equal PRE values. Second, it so happens that the elements that are most potent in preventing pitting can form precipitates, whereby local depletion may occur with associated passivity breakdown. The effects of such microstructural features will be discussed below.

In DSS local corrosion attack most frequently occurs at the austenite/ferrite phase boundaries.[29,75,76] This may be because the phase boundaries are preferential sites for segregation of impurities but since modern DSS are extremely clean, with sulphur contents of the order of 0·0015% or less this effect is considered to be less important. When phase transformations occur in the grain boundary regions, passivity breakdown can be explained by associated local chromium gradients. This was found to occur in duplex AISI 308 steel, which was heat treated to precipitate $M_{23}C_6$ particles at the austenite/ferrite boundaries.[77,78] Pitting resistance was evaluated by potentiodynamic and galvanostatic tests in 0·1M NaCl, in which localised attack was observed in the chromium depleted austenite adjacent to the precipitates. In a recent investigation[29] on SAF 2507, the simultaneous precipitation of Cr_2N, χ phase, and secondary austenite during isothermal aging at 800°C was found to initiate a large number of pits in the secondary austenite close to the prior austenite/ferrite boundaries. This could be directly related to the experimental observation of the secondary austenite being low in chromium (21% in the secondary austenite and 24% in the primary austenite). Similar conclusions were drawn in an investigation of U50, in which the chromium and molybdenum poor secondary austenite was formed within the grains.[24] However, the precipitation of σ phase is by far the most harmful transformation because of its high volume fraction and the associated depletion of the surrounding matrix with respect to chromium and molybdenum.[24,29,30,38,79–82]

Use is often made of DSS weld metal in joining low alloy steels to austenitic or duplex steels. Care must be exercised to avoid phase transformations during welding

that lead to decreased corrosion resistance. The rapid cooling often associated with welding may result in segregations or precipitation of chromium nitrides.[33,83] Insufficient shielding may cause nitrogen to escape from the weld.[84] All these effects have a detrimental influence on the pitting corrosion behaviour of DSS welds. This will be discussed in more detail in the 'Welding' section below.

STRESS CORROSION

Alloys that are subjected to the simultaneous action of corrosion and mechanical stress may fail by stress corrosion cracking.[2] The usual mode of cracking in DSS is transgranular but in sensitised steels, particularly austenitic steels, intergranular cracking can be observed.[85] Like pitting resistance, resistance to stress corrosion cracking (SCC) is dependent on a combination of the overall chemical composition and microstructure, although it seems that SCC is more sensitive to microstructure. All the evidence obtained to date shows that austenitic steels having moderate nickel contents are inherently more sensitive to SCC than are DSS. Figure 17 shows the SCC resistance for a selection of austenitic and duplex alloys obtained in oxygen bearing (about 0·0008%) neutral chloride solutions using a testing time of 1000 h at a stress equal to the yield stress at the testing temperature.[4] It is apparent in Fig. 17 that the low alloyed type 23Cr–4Ni DSS is superior to AISI 316 and AISI 304 austenitic steels. It can also be concluded from this diagram that the resistance to SCC in the DSS increases with additions of chromium and molybdenum. The super DSS is even superior to the highly alloyed Sanicro 28, which is a 27Cr–31Ni–3Mo austenitic alloy.

It has been shown that the resistance to SCC can be improved by increasing the volume fraction of ferrite in a DSS.[86] This is intimately related to the fact that the yield strength of the ferritic component often exceeds that of austenite, which is often reflected as a blocking of transgranular cracks at ferrite grains.[87] At low stress levels, Hochmann *et al.*[88] concluded that deformation is confined to the austenite and the ferrite is left virtually undeformed. They considered crack propagation under stress corrosion to be plastic deformation followed by slip dissolution. Clarke and Gordon[85] investigated DSS at higher stresses in high purity water at 288°C and found the DSS to be superior to the austenitic steels of type 304 also under these more severe conditions. In fact, the DSS 3RE60 did not even fail at stresses as high as twice the yield stress.

At high stresses and in very aggressive chloride ion containing media, the DSS do exhibit SCC failures. This was observed in an investigation of duplex AISI 329 in 0·1M NaCl at 300°C under constant loading[89] and in low strain rate tests at room temperature (RT) in 1M HCl of AISI 304 weld metal containing varying amounts of δ ferrite.[90] Particularly severe conditions have been found in chloride containing media in which either the pH value is low or H_2S is added. However, DSS having a molybdenum content of about 3% and above show satisfactory behaviour in hydrogen sulphide/chloride environments.[91] This has been confirmed by laboratory tests combined with successful long term service performance in sour environments containing H_2S.

On a general note it is worth pointing out that laboratory data must be interpreted with some caution since they are often obtained from accelerated tests and it is therefore not always known to what extent they simulate practical service conditions. Furthermore, the relative ranking of alloys is very sensitive to the type of environment employed. This was elucidated by Jargelius *et al.*[92] in a recent investigation on a series of DSS ranging from 23Cr–4Ni to 25Cr–7Ni–4Mo. However, as demonstrated in the investigations quoted above and also reflected in Fig. 17, the DSS are with few exceptions more resistant to SCC than austenitic steels of similar chromium and molybdenum content.

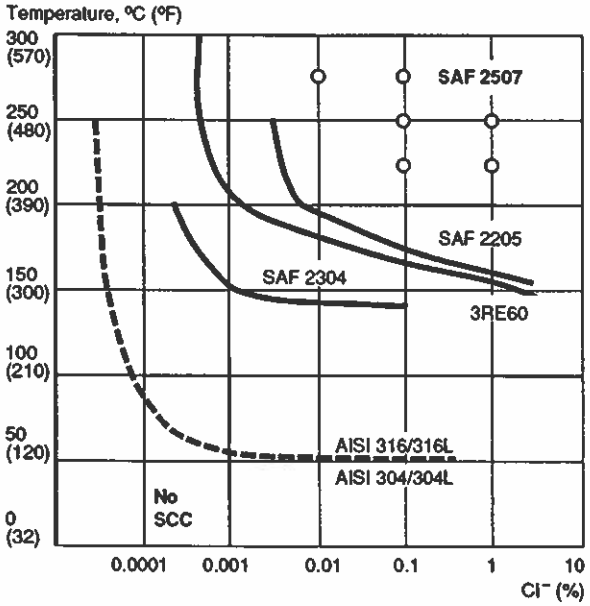

17 Stress corrosion cracking resistance in oxygen bearing neutral chloride solutions using testing time of 1000 h: applied stress was equal to yield stress during testing (From Ref. 4)

SENSITISATION

Sensitisation, which can occur after localised corrosion in the form of intergranular attack, is due to chromium depletion of the matrix surrounding intergranular carbides. These carbides are usually of the type $M_{23}C_6$, which precipitate during heat treatment in the temperature range 600–1000°C. This phenomenon is less pronounced in DSS than in austenitic steels for the following reasons. First, chromium is essentially supplied by the ferrite, in which diffusion is faster than in austenite, and as a result the chromium depleted zone becomes broader and more shallow in the ferrite.[78] Moreover, rapid healing of the comparatively narrow chromium depleted zone in austenite can be achieved in DSS owing to faster replenishment of chromium in depleted zones during prolonged aging treatments. Second, the carbon content of modern DSS is usually so low that precipitation of grain boundary carbides is suppressed. For example, in SAF 2507, which has a carbon content usually less than 0·015%, no carbides of any type have been observed although careful microscopic investigations have been performed.[29] Thus, the low carbon content in combination with the presence of ferrite reduces the problem of sensitisation to a negligible level in modern DSS.

Welding

Use is made of DSS weld metal in joining DSS and producing corrosion resistant overlays on low alloy steels. Because duplex filler metals are usually richer in alloying elements than the corresponding parent metal they tolerate substantial dilutions and still maintain a ferritic solidification mode. They are therefore suitable as filler metals in dissimilar joints between DSS and low alloy steels. However, the most common situation is the joining of two duplex components and the following discussion will be confined to this subject.

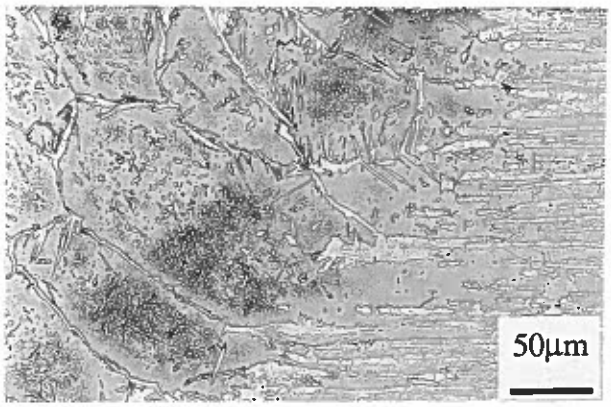

18 Light optical micrograph of chromium nitrides formed in heat affected zone after tungsten inert gas (TIG) welding in combination with rapid cooling of SAF 2507 (From Ref. 97)

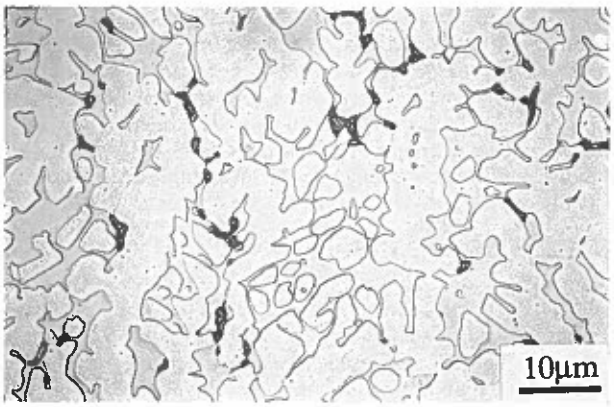

19 Light optical micrograph of σ phase formed in weld of SAF 2507 after high heat input TIG welding

Considerable progress has been achieved over the past decade as regards welding of DSS and the conditions for successful welding are now well defined (e.g. *see* Refs. 84, 93, and 94). Advances have been made by adjusting the chemical composition of the weld metal and the parent metal, and by optimising the welding parameters.[95–97] In doing so it has been essential to establish structure–property relations for a wide range of welding conditions.

Early DSS, in which the carbon content was sometimes as high as 0·10%, were susceptible to the formation of carbides.[98] It was virtually impossible to avoid carbide precipitation in the heat affected zone when welding such steels and as a result, a weld with low toughness and low corrosion resistance was produced. Moreover, the ferrite content in these steels was usually higher and this often resulted in entirely ferritic welds. In contrast, modern DSS are poor in carbon but rich in nitrogen. This implies that carbide formation is virtually eliminated and, owing to the high diffusivity of austenite stabilising nitrogen, welds of high toughness can be obtained by ready reformation of austenite. However, some caution is required since excess nitrogen in the ferrite may cause precipitation of chromium nitrides at high cooling rates. Furthermore, welding generates a heat affected zone, a region that can be regarded as a chill casting, and residual stresses, all of which may influence the properties.[99]

The heat affected zone (HAZ) is subjected to thermal cycles with peak temperatures ranging from near RT up to the melting point in regions close to the weld. Moreover, the cooling and heating rates may vary significantly with heat input, structural dimensions, and position relative to the weld. The situation is further complicated by the fact that multipass welding leads to repeated heating and cooling, the rates of which are very much dependent on the interpass temperature. As in other steels, the weld itself is sensitive to segregation of impurities because of the cast structure, and repeated heating can cause microstructural changes. Built-in stresses are expected to have an influence primarily on stress corrosion. The implications of microstructural changes on corrosion properties and mechanical properties are discussed below.

EFFECTS OF WELDING ON CORROSION AND MECHANICAL PROPERTIES

Simulation of thermal cycles occurring in the HAZ (*see* Fig. 18) has shown that very rapid cooling results in the formation of chromium nitrides with a small reduction in pitting resistance but virtually no reduction in impact toughness.[33] Similar results regarding pitting were found in the base metal HAZ produced by low heat input welding.[100] It is important to note that the susceptibility to nitride formation is reduced in high nitrogen containing DSS, in which nitrogen facilitates the reformation of austenite that, in turn, accommodates the majority of the nitrogen.[84]

The most deleterious precipitate to form is perhaps σ phase, which can precipitate in regions of the HAZ and the weld metal after excessively high heat input in combination with low cooling rates. An example of σ phase in the HAZ is shown in Fig. 19. It has been found that σ phase reduces the corrosion resistance[97,101] and, as for isothermally formed σ phase, welding induced σ phase can be expected to reduce toughness.

Reheating of large metastable ferrite grains may lead to the precipitation of an intragranular fine dispersion of secondary austenite, an example of which is shown in Fig. 20. This secondary austenite, which is sometimes found in reheated weld beads, has been found to be detrimental to pitting resistance,[95] presumably because it is poor in chromium and molybdenum.[24] As in the case of chromium nitrides, secondary austenite is avoided by alloying with nitrogen, which promotes the formation of primary austenite.

The value of the parameter Cr_{eq}/Ni_{eq}, where Cr_{eq} and Ni_{eq} are the chromium and nickel equivalents, respectively, seems to be critical in determining the mode of solidification during welding.[102] Below a certain value fully ferritic solidification occurs whereas above this value a combination of duplex and fully ferritic solidification is observed. The critical value of this parameter, as defined by Hammar and Svensson,[103] was found to be 2·25 in super DSS weld metals.[96] It has been shown that fully ferritic solidification

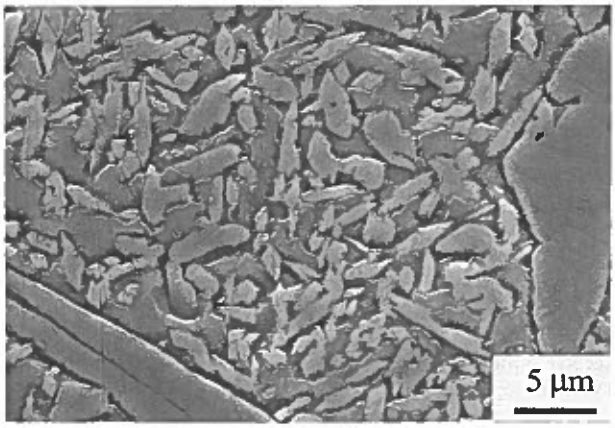

20 Secondary austenite formed in lower beads during multipass welding using 25Cr–10Ni–4Mo filler metal (SEM)

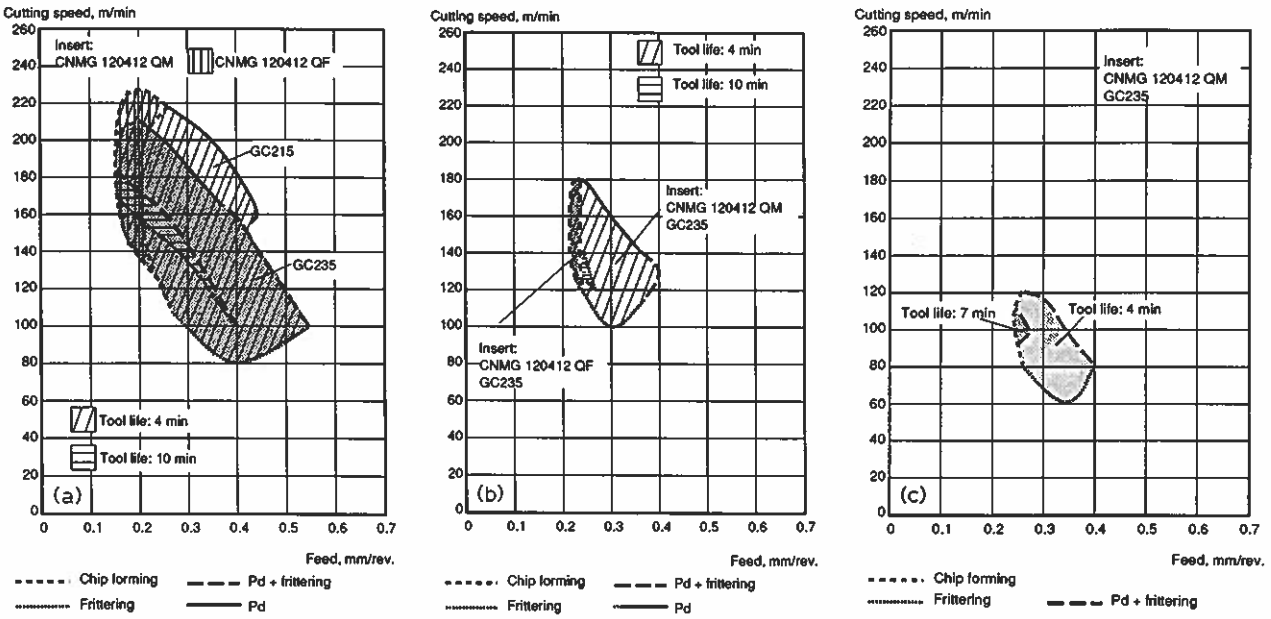

21 Machinability diagrams for *a* SAF 2304, *b* SAF 2205, and *c* SAF 2507, with recommended cutting insert indicated: key gives limiting mechanisms – Pd denotes plastic deformation (From Ref. 109)

is to be preferred since the resulting structure then achieves a higher toughness.[96] The adverse effects of mixed mode solidification derive from partitioning of chromium and molybdenum to ferrite and high energy interfaces deviating from the usual Kurdjumov–Sachs orientation, both of which enhance σ phase formation. This σ phase precipitated in regions of vermicular ferrite similar in morphology to the ferrite observed in type 304 welds by Baeslack *et al.*,[90] who observed that this ferrite was particularly sensitive to corrosion attack.

It should be borne in mind that, because of the comparatively high content of nickel in DSS filler metals, the partitioning of chromium and molybdenum to ferrite is more pronounced than in the corresponding base alloy. This implies that the C curves of intermetallic phases are displaced towards shorter times. Investigations of filler metals of the type 22Cr–8Ni–3Mo have shown the conditions for precipitation of R phase, χ phase, and σ phase in the range 600–1000°C (Refs. 35 and 104). Karlsson *et al.*[104] concluded that, provided the upper limit of the recommended range of heat input in super DSS (0·5–1·5 kJ mm^{-1}) is not exceeded, embrittlement due to precipitation of intermetallic phases will be eliminated. In tungsten and copper alloyed super DSS, however, the upper limit of the recommended range of heat input is as low as 1 kJ mm^{-1} when welding thin sections. This is supported by practical experience that such DSS are more sensitive to high heat inputs.[105] It is highly likely that the presence of tungsten, which has been observed to enhance precipitation kinetics under isothermal conditions,[8] is a contributing factor.

The equilibrium volume fraction of austenite will never be attained in a weld because of fast cooling. This is compensated for in part by the higher nickel content of the filler metal and the high mobility of nitrogen, but precautions must be taken to avoid excessively rapid cooling and low heat inputs. Recently developed models allow the prediction of the microstructure obtained for a given thermal cycle in terms of ferrite/austenite ratio[106,107] and grain growth,[108] and the resulting toughness can therefore usually be estimated.

In summary, it can be concluded that modern DSS can be successfully welded provided the recommended welding procedures are followed. Excessively rapid cooling may result in high volume fractions of ferrite, chromium nitrides, and secondary austenite, whereas slow cooling may lead to precipitation of intermetallic phases. Experience obtained in welding DSS has shown that the lower limit of the recommended range of heat input obtained at high cooling rates is the most critical. It is particularly important that this be taken into consideration when thick sections are to be welded.

Machinability

Good machinability is essential to the manufacturer of steel products because of its implications for productivity. The term machinability is very broad, involving various operations such as turning, drilling, cutting, and threading. It is widely known that DSS are more difficult to machine than standard austenitic steels. This is in part related to the higher strength of the DSS but other factors such as the low volume fraction of non-metallic inclusions and the low carbon content in modern DSS also contribute.

The machinability of steels can be improved and controlled by the introduction of non-metallic inclusions. Advantage has been taken of this effect in DSS of the type 22Cr–5Ni–3Mo by increasing the sulphur content.[109] However, an inevitable consequence of this is that corrosion resistance and toughness are reduced. In other words, a steel which is optimised for machining operations is usually not optimised with respect to corrosion properties and vice versa. Therefore, good corrosion resistance in DSS requires a compromise as regards machinability.

Extensive work has been performed to characterise the conditions necessary for good machinability in the standardised DSS SAF 2304, SAF 2205, and SAF 2507.[109,110] The results are often presented in diagrams where the abscissa represents feed and the ordinate represents cutting speed, and a shaded area displays the field of good machinability. Typical diagrams for these DSS are shown in Fig. 21, in which information concerning the recommended type of cemented carbide cutting insert is also given together with tool life recorded during the tests. A general conclusion to be drawn from these investigations is that the field of good machinability is reduced for increasing amounts of alloying elements. Experience has shown that molybdenum has a particularly

detrimental effect in this respect in both DSS and austenitic steels.

Although machinability is a complex field and many problems remain to be solved, some general comments can be made concerning the mechanisms that impose limitations on the machinability of DSS. At high cutting speeds, plastic deformation, involving flaking of the insert coating and frittering, is observed. Chip hammering can also be a problem under these conditions. At low cutting speeds, built-up edges causing flaking and frittering seem to be the limiting factor. When a large feed is used plastic deformation involving frittering occurs, whereas chip breaking becomes difficult when the feed is small. These limitations are qualitatively the same for all DSS although it must be pointed out that the highest tolerable cutting speed is significantly reduced for the high alloy steels.

In summary, DSS having a low volume fraction of non-metallic inclusions and optimised for corrosion resistance have reduced machinability. However, the conditions for good machining in DSS have been established in turning tests and are now well known.

Applications

Before DSS were introduced onto the market, the only alternatives to AISI 304 and 316 austenitic steels in aggressive environments were the expensive nickel rich austenitic steels. Experience from the past two decades has shown that the DSS provide alternatives that are not only more corrosion resistant than the austenitic grades but also low in expensive nickel. As a result of this, in combination with mechanical strength, toughness, and good weldability, they are suitable for many applications, particularly in chloride containing media. It is of course possible to find other types of steel that are superior to the DSS in one single respect, but the combination of the above mentioned properties shown by DSS is often outstanding.

The DSS have earned a place in the chemical, petrochemical, pulp and paper, power, and oil and gas industries. The biocompatibility of DSS having high PRE values has also been demonstrated and they are now used as implantation material in the human body.[111] It is not appropriate in a review of this nature to include a full description of the large number of varied applications in these areas. The reader who is interested in detailed information concerning applications and service experience is directed to the literature[112–120] and to the data sheets provided by the producers. However, the survey of different applications given in Table 4, which is by no means exhaustive, may serve as a guide for the reader. In an attempt to list the applications in a more systematic manner the DSS shown in Table 4 are grouped according to their resistance to pitting (PRE number), but it should be emphasised that other factors such as weldability and mechanical properties can be equally important in alloy selection.

Concluding remarks

Experience has shown that there is always a certain 'incubation' period from the time of market introduction of a new alloy to the general acceptance among end users. For DSS this is in part explained by the initial difficulties in welding the carbon rich DSS that were first introduced. However, the welding problem in modern DSS has now been overcome to the extent that welds can be produced that have corrosion and mechanical properties that are almost as good as those of the base material. This has been achieved by a combination of alloy design and development of welding procedures.

When appropriately treated, the DSS are unrivalled in a large number of applications in the temperature range −50 to 250°C where a combination of corrosion resistance and mechanical strength is required. However, the duplex microstructure, which is the key to the unique properties, also renders them inherently sensitive to phase transformations that may lead to reduced toughness and/or corrosion properties. Correct heat treatment and welding requires a thorough knowledge of the relationship between microstructural phenomena and properties. It is therefore essential for steel producers to convey this knowledge to manufacturers and users. In this paper much attention has been paid to deleterious phenomena such as the precipitation of undesirable phases of various types. In conjunction with this, the conditions for avoiding these phase transformations are defined and it is therefore hoped that this review article provides a basis for the successful use of DSS.

Acknowledgments

This paper is published with the permission of AB Sandvik Steel. The comments on the manuscript by the author's colleagues at Sandvik Steel Research and Development have been of invaluable help. In particular, the encouragement of Dr H. Widmark, and the assistance of Mr A. Wilson in calculating the phase diagrams are gratefully acknowledged.

Table 4 Applications of DSS in various industrial sectors

Industrial sector	23Cr–4Ni–0·1Mo, PRE = 25	22Cr–5Ni–3Mo, PRE = 30–36	25Cr DSS, PRE = 32–40	25Cr super DSS, PRE > 40
Chemical	Piping, instrumentation tubing	Pumps, fans, centrifuges, sulphur melting coils, chemical tankers	Urea strippers, reactor agitators, heat exchangers	Salt evaporation tubing, pumps, amine equipment, sea water cooling systems
Petrochemical	Tubular reactors where carbon steel shell is used	Various units for desalination, desulphurisation, and distillation	Pump casings, desulphurisation equipment	Tubes and pipes in Cl^- and HCl environments
Pulp and paper	Digester preheater, evaporators	Digesters in sulphate and sulphite plants	Digesters, digester preheaters	Bleaching equipment
Power generation (nuclear and fossil)	Feed water heaters, reheaters	Injection pipe in geothermal wells	...	Heat exchangers and systems in geothermal wells and saline brines
Oil and gas	Coolers, piping systems, tensioning systems, instrumentation tubing	Flare boom, framework, slotted oil liners, wirelines	Diving bells, pumps	Sea water cooling systems, fire water piping, pumps, pressure vessels, valve blocks

References

1. E. C. BAIN and W. E. GRIFFITHS: *Trans. AIME*, 1927, **75**, 166.
2. L. COLOMBIER and J. HOCHMANN: 'Aciers inoxydable aciers réfractaire'; 1955, Paris, Dunod.
3. C. EDELEANU: *J. Iron Steel Inst.*, 1953, **173**, 140–146.
4. S. BERNHARDSSON: Proc. Conf. 'Duplex stainless steels '91', 185; 1991, Les Ulis, France, Les Editions de Physique.
5. S. KARLSSON: Proc. Conf. 'Stainless steels '84', 438; 1985, London, The Institute of Metals.
6. R. KIESSLING and S. BERNHARDSSON: Proc. Conf. 'Duplex stainless steels '91', 605; 1991, Les Ulis, France, Les Editions de Physique.
7. H. D. SOLOMON and T. M. DEVINE: Proc. Conf. 'Duplex stainless steels', (ed. R. A. Lula), 693; 1984, Materials Park, OH, ASM.
8. J. CHARLES: Proc. Conf. 'Duplex stainless steels '91', 3; 1991, Les Ulis, France, Les Editions de Physique.
9. G. HERBSLEB: *Werkst. Korros.*, 1982, 33.
10. T. J. GLOVER: *Anti-Corrosion Methods Mater.*, 1982, **3**, 29.
11. J. W. PUGH and J. D. NISBET: *Trans. AIME*, 1950, **188**, 268.
12. L. COLOMBIER and J. HOCHMANN: 'Stainless and heat resisting steels'; 1968, New York, St. Martin's Press.
13. B. SUNDMAN, B. JANSSON, and J.-O. ANDERSSON: *Calphad*, 1985, **9**, 153.
14. Y. MAEHARA: *Trans. Iron Steel Inst. Jpn*, 1987, **27**, 705.
15. W. B. HUTCHINSON, K. USHIODA, and G. RUNNSJÖ: *Mater. Sci. Technol.*, 1985, **1**, (9), 728–731.
16. E. O. HALL and S. H. ALGIE: *Metall. Rev.*, 1966, **11**, 61.
17. S. ERIKSSON: *Jernkontorets Ann.*, 1934, **118**, 530.
18. J. S. KASPER: *Acta Metall.*, 1954, **2**, 456.
19. S. RIDEOUT, W. D. MANLEY, E. L. KAMEN, B. S. LEMENT, and P. A. BECK: *Trans. AIME*, 1951, **191**, 872.
20. D. A. EVANS and K. H. JACK: *Acta Crystallogr.*, 1957, **10**, 769.
21. A. REDJAIMIA, G. METAUER, and M. GANTOIS: Proc. Conf. 'Duplex stainless steels '91', 119; 1991, Les Ulis, France, Les Editions de Physique.
22. A. ROUAULT, P. HERPIN, and R. FRUCHART: *Ann. Chim.*, 1970, **5**, 461.
23. A. L. BOWMAN, G. P. ARNOLD, E. K. STORMS, and N. G. NERESON: *Acta Crystallogr. B*, 1972, **28**, 3102.
24. H. D. SOLOMON and T. M. DEVINE: 'Influence of microstructure on the mechanical properties and localised corrosion of a duplex stainless steel', STP 672, 430; 1979, Philadelphia, PA, ASTM.
25. P. JOLLY and J. HOCHMANN: *Mém. Sci. Rev. Métall.*, 1973, 117.
26. D. J. KOTECKI: *Weld. Res. Suppl.*, 1989, 431.
27. Y. MAEHARA, Y. OHMORI, J. MURAYAMA, N. FUJINO, and T. KUNITAKE: *Met. Sci.*, 1983, **17**, 541–547.
28. Y. MAEHARA, Y. OHMORI, and T. KUNITAKE: *Met. Technol.*, 1983, **10**, 296–303.
29. J.-O. NILSSON, A. WILSON, B. JOSEFSSON, and T. THORVALDSSON: Proc. Conf. 'Stainless steels '92', Stockholm, 9–11 June 1992, The Institute of Materials, Vol. 1, p. 280.
30. B. JOSEFSSON, J.-O. NILSSON, and A. WILSON: Proc. Conf. 'Duplex stainless steels '91', 67; 1991, Les Ulis, France, Les Editions de Physique.
31. Y. MAEHARA, N. FUJINO, and T. KUNITAKE: *Trans. Iron Steel Inst. Jpn*, 1983, **23**, 247.
32. J. HOCHMANN, A. DESESTRET, P. JOLLY, and R. MAYOUD: *Mét. Corr. Industrie*, 1974, **2**, (591–592), 390.
33. S. HERTZMAN, W. ROBERTS, and M. LINDENMO: Proc. Conf. 'Duplex stainless steels', 257; 1986, The Hague, The Netherlands, Nederlands Instituut voor Lastechniek.
34. P. D. SOUTHWICK and R. W. K. HONEYCOMBE: *Met. Sci.*, 1980, **14**, 253–261.
35. J.-O. NILSSON and P. LIU: *Mater. Sci. Technol.*, 1991, **7**, (9), 853–862.
36. J. HOCHMANN, A. DESESTRET, P. JOLLY, and R. MAYOUD: *Mét. Corr. Industrie*, 1974, **2**, (591–592), 404.
37. P. D. SOUTHWICK and R. W. K. HONEYCOMBE: *Met. Sci.*, 1982, **16**, 475–481.
38. T. THORVALDSSON, H. ERIKSSON, J. KUTKA, and A. SALWÉN: Proc. Conf. 'Stainless steels '84', 101; 1985, London, The Institute of Metals.
39. B. SOYLU and R. W. K. HONEYCOMBE: *Mater. Sci. Technol.*, 1991, **7**, (2), 137–145.
40. R. LAGNEBORG: *Trans. ASM*, 1967, **60**, 67.
41. M. COURTNALL and F. B. PICKERING: *Met. Sci.*, 1976, **10**, 273–276.
42. S. HERTZMAN: 'Influence of spinodal decomposition on impact strength of SS 2377 duplex stainless steel weldments', Internal Report, Swedish Institute for Metals Research, Stockholm, 1989, to be released.
43. G. WAHLBERG: PhD dissertation, Chalmers University of Technology, Gothenburg, Sweden, 1989.
44. M. K. MILLER and J. BENTLEY: *Mater. Sci. Technol.*, 1990, **6**, (3), 285–292.
45. J. E. BROWN, A. CEREZO, T. J. GODFREY, M. G. HETHERINGTON, and G. D. W. SMITH: *Mater. Sci. Technol.*, 1990, **6**, (3), 293–300.
46. P. AUGER, F. DANOIX, A. MENAND, S. BONNET, J. BOURGOIN, and M. GUTTMANN: *Mater. Sci. Technol.*, 1990, **6**, (3), 301–313.
47. M. GUTTMANN: Proc. Conf. 'Duplex stainless steels '91', 79; 1991, Les Ulis, France, Les Editions de Physique.
48. R. O. WILLIAMS: *Trans. AIME*, 1958, **212**, 497.
49. M. HILLERT: *Acta Metall.*, 1961, **9**, 525.
50. J. W. CAHN: *Trans. AIME*, 1968, **242**, 166.
51. A. HENDRY, Z. F. MAZUR, and K. H. JACK: *Met. Sci.*, 1979, **13**, 482–486.
52. A. WILSON: 'Estimation of impact toughness as a function of aging temperature and time', Internal Report no. 6079, Sandvik Steel, Sandviken, Sweden, 1991.
53. S. FLOREEN and H. W. HAYDEN: *Trans. ASM*, 1968, **61**, 489.
54. H. W. HAYDEN and S. FLOREEN: *Trans. ASM*, 1968, **61**, 474.
55. R. E. SMALLMAN: 'Modern physical metallurgy', 263; 1985, London, Butterworth.
56. M. NYSTRÖM, B. KARLSSON, and J. WASÉN: Proc. Conf. 'Stainless steels '91', Chiba, Japan, 10–13 June 1991, The Iron and Steel Institute of Japan, p. 738.
57. R. JOHANSSON and J.-O. NILSSON: Proc. Conf. 'Stainless steels '84', 446; 1985, London, The Institute of Metals.
58. H. D. SOLOMON and E. KOCH: *Scr. Metall.*, 1979, **13**, 1971.
59. P. NORBERG: Proc. Conf. 'Duplex stainless steels', 298; 1986, The Hague, The Netherlands, Nederlands Instituut voor Lastechniek.
60. R. MATHIS: *J. Mater. Sci.*, 1987, **22**, 907.
61. A. ATRENS: *Met. Technol.*, 1982, **9**, 117–121.
62. T. MAGNIN, J. M. LARDON, and L. COUDREUSE: 'A new approach to low cycle fatigue behaviour of a duplex stainless steel based on the deformation mechanisms of the individual phases', STP 942, 812; 1988, Philadelphia, PA, ASTM.
63. M. JACOBSSON: 'Fatigue testing of the duplex grades SAF 2304, SAF 2205 and SAF 2507', Internal Report no. 6060, Sandvik Steel, Sandviken, Sweden, 1991.
64. J. MOSKOVITZ and R. PELLOUX: 'Corrosion fatigue technology', STP 642, 133; 1978, Philadelphia, PA, ASTM.
65. H. W. HAYDEN and S. FLOREEN: *Metall. Trans.*, 1973, **4**, 561.
66. A. G. HAYNES: 'Duplex and high alloy corrosion resisting steels' Lloyd's Register Technical Association paper no. 6. 1990–1991, p. 1.
67. M. SPEIDEL: Proc. 6th Int. Conf. on Fracture, Vol. 1, 379; 1984, Oxford, Pergamon Press.
68. R. E. JOHANSSON and H. L. GROTH: Proc. Conf. 'Duplex stainless steels '91', 283; 1991, Les Ulis, France, Les Editions de Physique.
69. T. J. MARROW, C. A. HIPPSLEY, and J. E. KING: *Acta Metall. Mater.*, 1991, **39**, 1367.
70. P. COMBRADE and J.-P. AUDOUARD: Proc. Conf. 'Duplex stainless steels '91', 257; 1991, Les Ulis, France, Les Editions de Physique.
71. K. LORENTZ and G. MEDAWAR: *Thyssen Forschung*, 1969, **1**, 97.
72. J. CHARLES, J.-P. AUDOUARD, R. BLONDEAU, and P. SOULIGNAC: Proc. Conf. 'Stainless steels '91', Chiba, Japan, 10–13 June 1991, The Iron and Steel Institute of Japan, p. 1077.
73. M. B. ROCKEL and M. RENNER: *Werkst. Korros.*, 1984, **35**, 537.
74. ASTM G48, Annual Book of ASTM Standards, Sec. 3, 178; 1991, Philadelphia, PA, ASTM.
75. P. E. MANNING, D. J. DUQUETTE, and W. F. SAVAGE: *Corrosion*, 1979, **35**, 151.
76. P. HRONSKY and D. J. DUQUETTE: *Corrosion*, 1982, **38**, 63.
77. T. M. DEVINE: *J. Electrochem. Soc.*, 1979, **126**, (3), 374.
78. T. M. DEVINE and B. J. DRUMMOND: *Corrosion*, 1981, **37**, (2), 104.

79. S. HERTZMAN, B. LEHTINEN, and E. SYMNIOTIS-BARRDAHL: 'Intermetallic phase formation and its effect on corrosion resistance of duplex stainless steel UNS 31803', Internal Report no. 2703, Swedish Institute for Metals Research, Stockholm, 1991.
80. C. HONGLU and S. HERTZMAN: 'Kinetics of intermetallic phase formation in duplex stainless steels and their influence on corrosion resistance', Internal Report no. 2689, Swedish Institute for Metals Research, Stockholm, 1991.
81. G. HERBSLEB and P. SCHWAAB: Proc. Conf. 'Duplex stainless steels', 15; 1984, Metals Park, OH, ASM.
82. A. J. SEDRIKS: *Corrosion*, 1989, **45**, 510.
83. S. HERTZMAN and E. SYMNIOTIS: 'Stainless steels '91', Chiba, Japan, 10–13 June 1991, The Iron and Steel Institute of Japan, p. 1085.
84. B. JOSEFSSON: 'Stainless steels '91', Chiba, Japan, 10–13 June 1991, The Iron and Steel Institute of Japan, p. 1069.
85. W. L. CLARKE and G. M. GORDON: *Corrosion*, 1973, **29**, (1), 1.
86. J. W. FLOWERS, F. H. BECK, and M. G. FONTANA: *Corrosion*, 1963, **19**, 186t.
87. S. SHIMODAIRA, M. TAKANO, Y. TAKIZAWA, and H. KAMIDE: Proc. Conf. 'Stress corrosion cracking and hydrogen embrittlement of iron base alloys', Vol. 5, 1003; 1973, Houston, TX, NACE.
88. J. HOCHMANN, A. DESESTRET, P. JOLLY, and R. MAYOUD: *Mét. Corr. Industrie*, 1975, **3**, 593, 1.
89. S. HENRIKSSON and M. ÅSBERG: *Corrosion*, 1979, **35**, (9), 429.
90. W. A. BAESLACK, D. J. DUQUETTE, and W. F. SAVAGE: *Corrosion*, 1979, **35**, (2), 45.
91. H. ERIKSSON and S. BERNHARDSSON: *Corrosion*, 1991, **47**, (9), 719.
92. R. F. A. JARGELIUS, R. BLOM, S. HERTZMAN, and J. LINDER: Proc. Conf. 'Duplex stainless steels '91', 211; 1991, Les Ulis, France, Les Editions de Physique.
93. L. van NASSAU, H. MEELKER, and J. HILKES: Proc. Conf. 'Duplex stainless steels '91', 303; 1991, Les Ulis, France, Les Editions de Physique.
94. B. LUNDQUIST: 'Welding of modern stainless steels', Sandvik Steel lecture S-9147, Sandviken, Sweden, 1989.
95. S. PAK and L. KARLSSON: *Scand. J. Metall.*, 1990, **19**, 9.
96. L. KARLSSON, S. PAK, and S. L. ANDERSSON: 'Stainless steels '91', Chiba, Japan, 10–13 June 1991, The Iron and Steel Institute of Japan, p. 1093.
97. S.-Å. FAGER: Proc. Conf. 'Duplex stainless steels '91', 403; 1991, Les Ulis, France, Les Editions de Physique.
98. F. R. BECKITT: *J. Iron Steel Inst.*, 1969, **207**, 632–638.
99. T. G. GOOCH: Proc. Conf. 'Duplex stainless steels '91', 325; 1991, Les Ulis, France, Les Editions de Physique.
100. L. KARLSSON and S. PAK: Proc. Conf. 'Duplex stainless steels '91', 413; 1991, Les Ulis, France, Les Editions de Physique.
101. D. FAUCHEUR and D. GILBERT: 'Duplex stainless steels', 83; 1986, The Hague, The Netherlands, Nederlands Instituut voor Lastechniek.
102. N. SUUTALA, T. TAKALO, and T. MOISIO: *Metall. Trans.*, 1979, **10A**, 1183.
103. Ö. HAMMAR and U. SVENSSON: Proc. Conf. 'Solidification and casting of metals', 401; 1979, London, The Metals Society.
104. L. KARLSSON, L. BENGTSSON, U. ROLANDER, and S. PAK: Proc. Conf. 'Stainless steels '92', Stockholm, 9–11 June 1992, The Institute of Materials, Vol. I, p. 335.
105. S. PAK and L. KARLSSON: 'Welding the super duplex stainless steel Zeron 100', Internal Report, Elektro svets aktiebolaget, Gothenburg, Sweden, 1992.
106. J. C. LIPPOLD, I. VAROL, and W. A. BAESLACK: Proc. Conf. 'Duplex stainless steels '91', 383; 1991, Les Ulis, France, Les Editions de Physique.
107. B. BONNEFOIS, J. CHARLES, F. DUPOIRON, and P. SOULIGNAC: Proc. Conf. 'Duplex stainless steels '91', 347; 1991, Les Ulis, France, Les Editions de Physique.
108. B. E. S. LINDBLOM, B. LUNDQUIST, and N. E. HANNERZ: Proc. Conf. 'Duplex stainless steels '91', 373; 1991, Les Ulis, France, Les Editions de Physique.
109. C.-G. CARLBORG, Å. NILSSON, and P.-Å. FRANKLIND: Proc. Conf. 'Duplex stainless steels '91', 685; 1991, Les Ulis, France, Les Editions de Physique.
110. P.-Å. FRANKLIND and C.-G. CARLBORG: Proc. Conf. 'Stainless steels '92', Stockholm, 9–11 June 1992, The Institute of Materials.
111. A. CIGADA, S. DeMARTIIS, G. RONDELLI, B. VINCENTINI, M. GIACOMAZZI, and A. ROOS: 'Stainless steels '91', Chiba, Japan, 10–13 June 1991, The Iron and Steel Institute of Japan, p. 716.
112. D. J. A. FRUYTIER: Proc. Conf. 'Duplex stainless steels '91', 497; 1991, Les Ulis, France, Les Editions de Physique.
113. C. DURET-THUAL and J. L. MOIRON: Proc. Conf. 'Duplex stainless steels '91', 511; 1991, Les Ulis, France, Les Editions de Physique.
114. C. COUSSEMENT and D. FRUYTIER: Proc. Conf. 'Duplex stainless steels '91', 521; 1991, Les Ulis, France, Les Editions de Physique.
115. R. L. RICHARD: Proc. Conf. 'Duplex stainless steels '91', 531; 1991, Les Ulis, France, Les Editions de Physique.
116. G. H. WAGNER and R. MÜNSTER: Proc. Conf. 'Duplex stainless steels '91', 541; 1991, Les Ulis, France, Les Editions de Physique.
117. M. LOZE, O. AGASSE, P. RICHARD, and F. HAEGELI: Proc. Conf. 'Duplex stainless steels '91', 551; 1991, Les Ulis, France, Les Editions de Physique.
118. B. LEFFLER: Proc. Conf. 'Duplex stainless steels '91', 567; 1991, Les Ulis, France, Les Editions de Physique.
119. L. FASSINA: Proc. Conf. 'Duplex stainless steels '91', 579; 1991, Les Ulis, France, Les Editions de Physique.
120. J. HILKES, K. BEKKERS, and H. MEELKER: Proc. Conf. 'Duplex stainless steels '91', 595; 1991, Les Ulis, France, Les Editions de Physique.